JOURNAL OF MATERIALS SCIENCE 24 (1989) 2503–2507

High-temperature properties of ferritic spheroidal graphite cast iron

T. S. LUI, C. G. CHAO
Department of Materials Engineering, National Cheng-Kung University, Tainan, Taiwan

The behaviour of fracture mode and intermediate temperature embrittlement of ferritic spheroidal graphite cast iron is influenced by many factors. From the experimental results, intermediate temperature embrittlement can be considered to be dominated by dynamic strain ageing and the triaxial stress field developed in the ferrite matrix amongst the graphite particles. In order to understand the effect of dynamic strain ageing on high-temperature properties, tensile properties, push–pull low-cycle fatigue properties, rotary bending fatigue properties and creep-rupture properties were investigated from room temperature to 500° C. It was found that all the properties investigated were influenced by dynamic strain ageing. The intermediate temperature embrittlement of ferritic spheroidal graphite cast iron found in different load conditions is reported.

1. Introduction

The ferritic spheroidal graphite cast irons exhibit their best ductility in cast irons. They can usually be applied at elevated temperature because the ferrite stable phase can be retained up to 600° C. However, very little work has been done on the high-temperature properties of ferritic spheroidal graphite cast irons, the exceptions being Chichiwa and Hayashi [1], Nechtelberger [2], and Lui and Yanagiswa [3], who have studied tensile and thermal fatigue properties. In order to study the high-temperature deformation and fracture behaviour under different load conditions of ferritic spheroidal graphite cast irons, the chemical composition, graphite morphology, and grain size were fixed, and only the stress conditions and test temperatures were varied. In addition, ferritic spheroidal graphite cast irons have exhibited serrations in the tensile stress–strain curve between 150 and 350° C. From previous experimental reports [1, 4], the serration was found to depend on dynamic strain ageing which was closely related to intermediate temperature embrittlement caused by intergranular fracture. The temperature ranges in these investigations were overlapped with the test temperature range of the serrations. Therefore, they are discussed together in order to understand the mechanism of embrittlement of ferritic spheroidal graphite irons.

2. Experimental procedure

The materials used in this study were melted in a 20 kg basic lined induction furnace from a charge of raw pig iron. A small compensating addition of electrolytic iron and ferrosilicon was made to the furnace throughout the heating process to adjust the composition. The iron was melted, brought to a suitable superheat of 1470° C, spheroidized with (1.1 wt %) Fe–45 wt % Si–4 wt % Mg alloy (KC4), and inoculated with (0.3 wt %) Fe–75 wt % Si alloy, then poured into a 60 mm × 100 mm × 300 mm CO_2 mould.

The materials were annealed to the ferritic state by keeping them at 930° C for 3 h, 720° C for 3 h, and cooling in a furnace, as shown in Fig. 1. The full ferrite microstructure is shown in Fig. 2. The ferrite grain size, graphite diameter, and graphite volume fraction were measured by quantitative analysis. The results are listed in Table I. Chemical compositions identified by emission spectrometry are listed in Table II.

The high-temperature tensile tests and low-cycle fatigue tests were carried out with an M.T.S. materials testing machine under the same heating conditions used in a previous report [3]. Parallel parts of the specimens for low-cycle fatigue were machined to dimensions of 8 mm × 15 mm, and the grip parts were machined into an M 12 × 1.75 mm screw thread. The strain amplitudes ($\Delta\varepsilon_p$) chosen were 0.5% and 1.0%. The creep rupture test was carried out using a creep machine. The specimens for this creep test were the same as those for the tensile test with parallel parts 6 mm × 30 mm. According to the results of the tensile test, a creep stress of 38 to 22 kg mm^{-2} was chosen depending on the temperature. The temperature variation in all high-temperature tests was controlled to ±3° C. The fracture surfaces were examined by scanning electron microscopy (SEM).

TABLE I Quantitative analysis of microstructure

Ferrite grain size (μm)	Graphite diameter (μm)	Graphite vol. fraction (%)
44	52	12.8

TABLE II Chemical compositions (wt %)

C	Si	Mn	P	S	Mg
3.53	2.80	0.012	0.035	0.002	0.050

0022–2461/89 $03.00 + .12

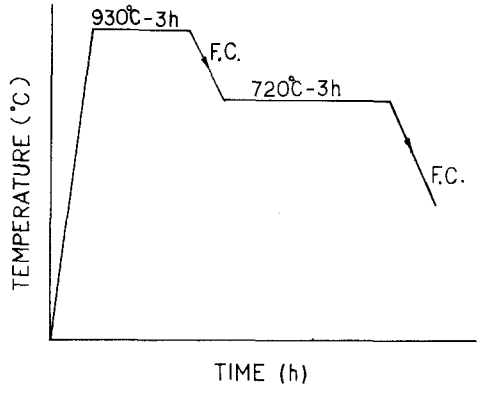

Figure 1 Heat-treatment conditions. F.C. = fast-cooled.

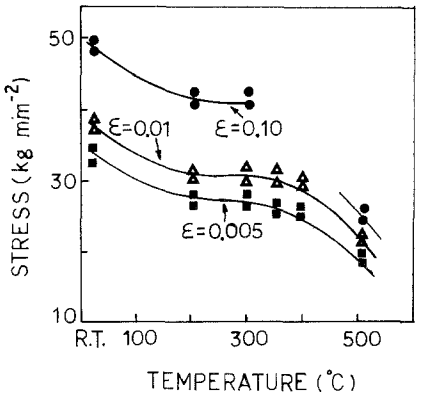

Figure 3 The relationship between flow stress and test temperature.

3. Results

3.1. Results of tensile tests at elevated temperature

Ferritic spheroidal graphite cast irons were tensile tested under 500° C. The flow stress could be obtained from the stress–strain curves at various strain levels, which could be used as a reference for other tests. Fig. 3 shows the relationship between flow stress and temperature from which it is seen that the flow stress of ferritic spheroidal graphite cast irons decreased with increasing temperature from room temperature to 200° C in the tensile tests. Nevertheless, a flow stress plateau was seen in the stress–strain curve from 200 to 350° C and the flow stress dropped sharply when the temperature rose above 400° C. This result is similar to other reports [5, 6].

Serrated flow was observed with a low strain rate ($\dot{\varepsilon} = 2.8 \times 10^{-4}\,\mathrm{sec}^{-1}$) in the interval between 150 and 350° C, which was due to dynamic strain ageing [1]. This phenomenon was relevant to fine carbide precipitates at higher temperatures [7], as well as the diffusion of interstitial atoms, such as carbon or nitrogen, at lower temperature. The relationship between elongation and temperature is shown in Fig. 4. Intergranular fracture occurred in ferritic spheroidal graphite cast irons on increasing the temperature from 300 to 400° C; the minimum ductility was at 400° C. This was due to dynamic strain ageing, such as the blue brittleness of steel in which solute atoms interacted with dislocations, but the temperature for minimum ductility differed [8], and only the dimple pattern could be observed. In general, with a similar strain rate ($10^{-4}\,\mathrm{sec}^{-1}$), the ductility of mild steel was severely reduced at temperatures between 200 and 250° C; even the 1% Si and 3% Si alloys had embrittlement temperatures around 300° C [9]. Cast Fe–2.6 wt % Si alloy (without graphite particles) had an embrittlement temperature between 300 and 350° C [10]. However, the ferritic spheroidal graphite cast iron had a higher embrittlement temperature, about 400° C. It is suggested that this may be because the ferritic spheroidal graphite cast irons had higher silicon and graphite particle contents. In addition, the change in fractography at high-temperature embrittlement was one of the most important factors. According to a previous report [8], the fracture surfaces of blue-brittle mild steel and Fe–Si alloy showed a dimple pattern, as did the fracture surfaces of Fe–2.6 wt % Si cast at the embrittlement temperature. Nevertheless, the cast Fe-2.6 wt % Si alloy specimen which was machine-notched showed the stress condition induced as a triaxial stress field, and the fracture surfaces changed from dimple pattern to intergranular fracture at 400° C. Clearly, the spheroidal graphite particles had an essential influence on the embrittlement, which shifted to higher temperatures, and the intergranular fracture which occurred [4, 10]. Fig. 5 shows (a) the dimple pattern at 300° C and (b) intergranular fracture at 400° C.

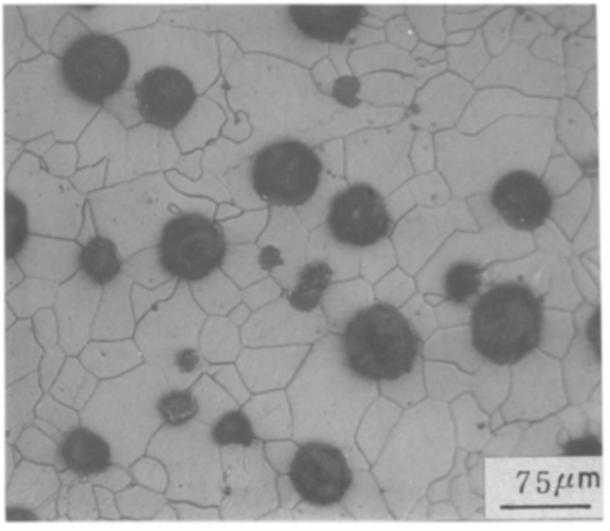

Figure 2 The microstructure of the specimens.

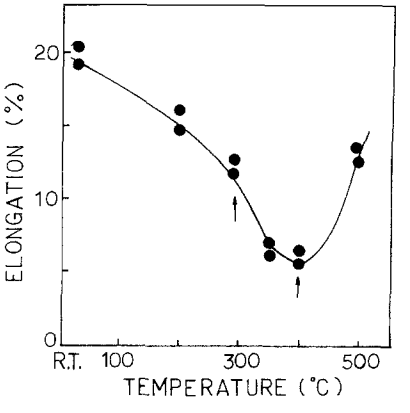

Figure 4 The relationship between elongation and test temperature.

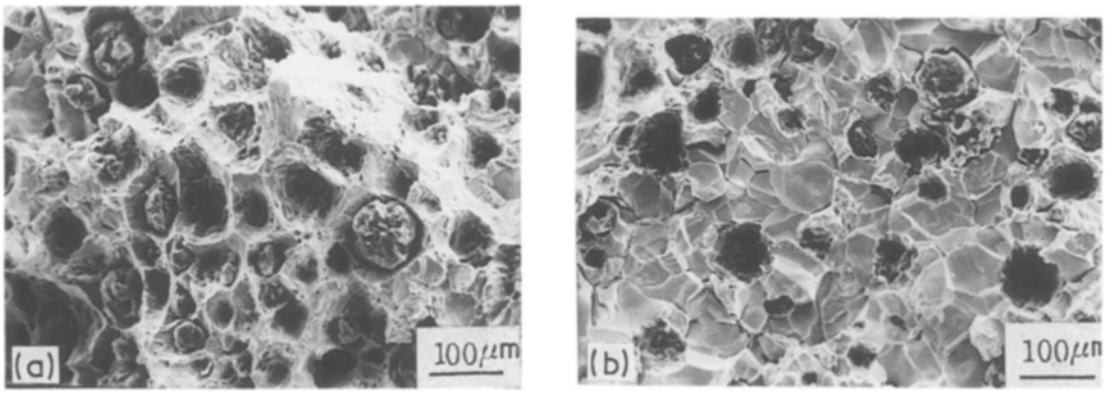

Figure 5 Scanning electron micrographs of the fracture surface of specimens at (a) 300° C, (b) 400° C.

3.2. Results of fatigue test at elevated temperature

The ferritic spheroidal graphite cast irons are usually subjected to high temperatures [2]. From the experimental results the effects of dynamic strain ageing and intergranular fracture under 500° C can be seen. It was worth studying whether the phenomenon would occur under different stress conditions, especially for fatigue properties at high temperatures. For example, studying the mechanism of brittleness of ferritic spheroidal graphite cast irons by means of rotary bending fatigue and push–pull low-cycle fatigue, was very interesting.

In the previous report the influence of graphite morphology on fatigue strength in the rotary bending fatigue test was shown [3]. It was pointed out that dynamic strain ageing influenced fatigue strength and had a close relationship with intergranular fracture during high-temperature fatigue. Fig. 6 shows that the number of cycles-to-failure decreased with increasing temperature. Fig. 7 shows that the fatigue limit (a), and fatigue lifetime strength (b) depend on temperature in the rotary bending fatigue tests. The fatigue strength did not monotonically decrease with increasing temperature implying that the fatigue strength increased by dynamic strain ageing between 150 and 350° C. The results of the push–pull low-cycle fatigue tests showed the same tendency between room temperature, 300, 400 and 500° C as shown in Fig. 8. We could determine the strain hardening rate in the initial stage by measuring the total stress which occurs with increasing the cycle numbers with constant strain. The total stress did increase due to strain hardening (σ_t included tension and compression). Above 10 push–pull cycles, the strain hardening rate no longer increased, and gradually became flat at room temperature and 500° C as shown in Fig. 8. Nevertheless, continuous strain hardening occurred until it fractured at 300° C (it could not be measured at 400° C). Jaske [11] pointed out that carbon steel exhibited the same phenomenon in regard to dynamic strain ageing.

Fig. 9 shows the effect of temperature on the number of cycles-to-failure in high-temperature low-cycle fatigue tests. Although the strain rates were different in the tensile and low-cycle fatigue tests, the minimum fatigue lifetime of low-cycle fatigue coincided at about 400° C. Furthermore, Fig. 9 shows that the fatigue lifetime decreases with increasing temperature and the curve undergoes an upwards inflection with temperatures above 400° C. In other words, this implies that the elongation was proportional to fatigue lifetime.

3.3. Results of creep rupture test

All the properties of tensile tests, rotary bending fatigue tests and the push–pull low-cycle fatigue tests mentioned above are relevant to dynamic strain ageing at intermediate temperatures. From this point of view, the creep rupture test in which the strain rate was very slow should show the same tendency. In particular, the intermediate temperature embrittlement

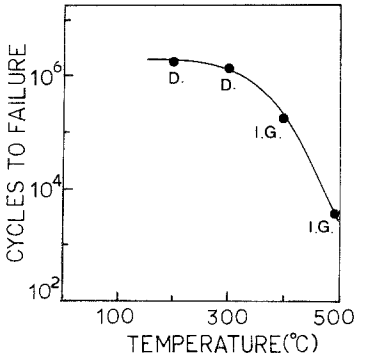

Figure 6 The influence of temperature on fractography and cycles-to-failure of the rotary bending fatigue test at 20 kg mm^{-2}. *D, dimple pattern; I.G. intergranular fracture.

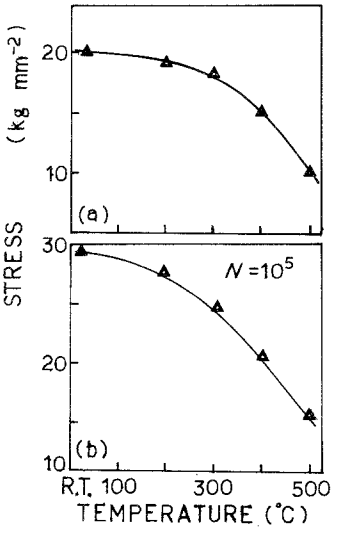

Figure 7 The influence of temperature on the rotary bending fatigue test: (a) fatigue limit, (b) fatigue lifetime strength.

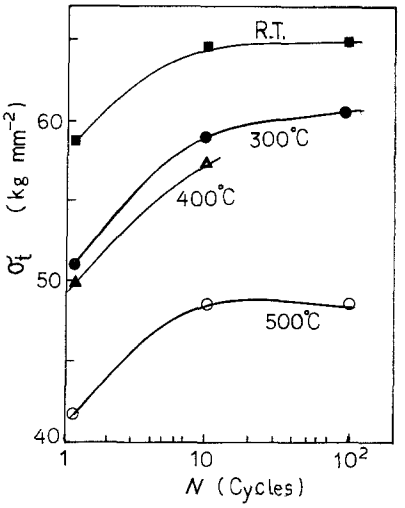

Figure 8 The correlation of the total stress and cycle number of the low-cycle fatigue tests at various temperatures.

and intergranular fracture of ferritic spheroidal graphite cast irons depended on strain rate according to Lui [7]. The phenomenon shifts to lower temperatures with decreasing strain rate.

Fig. 10 shows the correlation of stress with time-to-rupture in the creep rupture test. The time-to-rupture–creep stress plot shows a linear relationship with temperatures A (300° C), B (350° C), C (400° C), and D (450° C). The time-to-rupture decreased with increasing creep stress, the same as in common creep tests. Nevertheless, we calculated the elongation of specimens with various stress levels by measuring the gauge mark. The results are indicated in Fig. 11. The elongation decreased with decreasing temperature below 450° C; the temperature even dropping to 300° C without upwards inflection. Because the creep rupture test could be regarded as a tensile test with a very slow strain rate, it seems reasonable for the embrittlement temperature to shift to lower temperatures. A detailed discussion requires further study. In summary, under the different stress conditions, we have shown that the dynamic strain ageing which induced ferritic spheroidal graphite cast iron embrittlement, not only in the high-temperature tensile test, but also affected creep rupture and high-temperature fatigue properties.

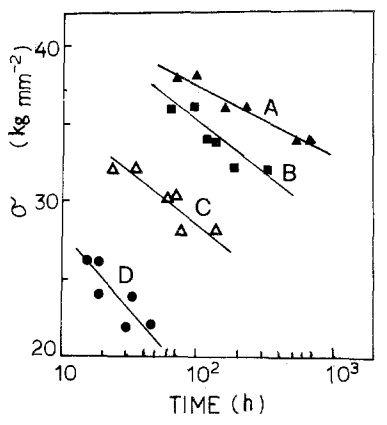

Figure 10 The correlation of stress with time-to-rupture in the creep test. A, 300° C; B, 350° C; C, 400° C; D, 450° C.

4. Discussion

From the different experimental results, the high-temperature properties of ferritic spheroidal graphite cast iron have emerged. No matter which test (tensile, rotary bending fatigue, push–pull low-cycle fatigue, or creep rupture) was used all exhibited intermediate temperature embrittlement. According to Chichiwa's [1] and Lui's [7] investigations on ferritic spheroidal graphite cast irons, Blackmore's [6], Omori's [12] and Takeyama's [8] investigations on mild steel, Sachdev's [13] and Abe's [14] investigations on ferro-carbon alloy, the serrated flow stress resulted from dynamic strain ageing which decreased the ductility of the material.

Lui and Yanagisawa [4] demonstrated that ferritic spheroidal graphite cast irons had diffusion-dependent intergranular fracture, and the relationship between strain rate ($\dot{\varepsilon}$) and temperature was linear in the tensile test, following the equation

$$\dot{\varepsilon} = A \exp\left(-\frac{H}{RT}\right)$$

However, the results explained in this study are worth further studying, because only the strain rate was changed in the tensile tests. Generally, the stress conditions of fatigue were different from those in the tensile tests. When materials underwent a cycle stress at high temperature, the situation was basically a combination of creep and fatigue. Therefore, the fatigue properties were very different between high

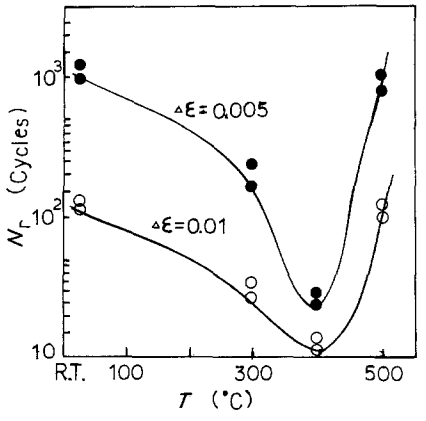

Figure 9 The effect of temperature on the number of cycles-to-fatigue in the low-cycle fatigue tests with $\Delta\varepsilon_p$ = 0.01 and 0.005.

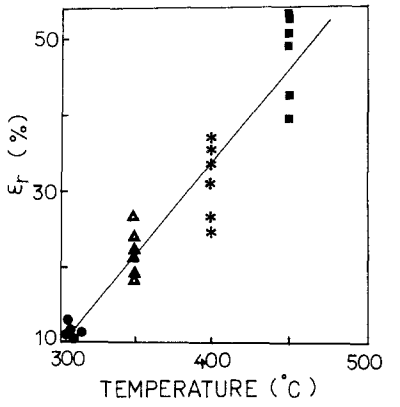

Figure 11 The influence of temperature on elongation in creep rupture tests.

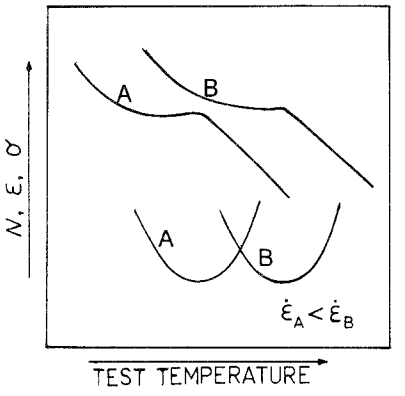

Figure 12 A schematic plot showing that the embrittlement range moved to higher temperatures with increasing strain rate.

temperature and room temperature. For example, generally the choice of cycle frequency in the fatigue test was 200 to 10 000 r.p.m. The fatigue strength was almost independent of cycle frequency at room temperature, but the cycle frequency had a strong influence on fatigue strength at high temperature. This implied that fatigue strength under the influence of strain rate shows the same trend as tensile strength [7]. In this study the rotary bending fatigue test employed a constant cycle speed (3000 r.p.m.) to avoid this problem. The results from push–pull low-cycle fatigue and creep rupture tests were compared with other tests in order to determine the effect of strain rate. In this study the stress conditions were different, but the results from Figs 3, 4 (tensile test), 6, 7 (rotary bending fatigue test), 8, 9 (low-cycle fatigue test) and 10 (creep rupture test) showed the brittleness range at 350 to 400° C in the tensile test, the minimum lifetime range also around 400° C in the low-cycle fatigue, the minimum lifetime with 20 kg mm^{-2} stress in rotary bending fatigue at 500° C, and in the meantime intergranular fracture mixing with a dimple pattern, in addition to minimum elongation at lower temperature (300° C) in the creep rupture test. Clearly, the high-temperature properties of ferritic spheroidal graphite cast irons have a close relationship with the dynamic strain ageing effect, which was a diffusion dominating phenomenon.

Fig. 12 shows a schematic plot in which the embrittlement range moves to higher temperatures with increasing strain rate; otherwise it moved to lower temperatures. It is well known that dynamic strain ageing affects the fatigue strength in carbon steel. The embrittlement temperature due to dynamic strain ageing was about 150 to 250° C, the ferritic spheroidal graphite cast irons showing the same tendency, their embrittlement temperatures being at higher temperatures (about 300 to 400° C). The reason for this is suggested to be that silicon contents were higher and spheroidal graphite particles were present.

5. Conclusions

The high temperature properties of ferritic spheroidal cast irons, were studied by high-temperature tensile, rotary bending fatigue, low-cycle fatigue at high temperature and creep rupture tests, and the results can be described as follows.

1. The high-temperature tensile properties of ferritic spheroidal graphite cast irons were affected by dynamic strain ageing. Under other load conditions serrated flow stress was not observed to result in dynamic strain ageing but the results did show a relationship to dynamic strain ageing.

2. All these tests at high temperature indicated one of the most important factors in inducing embrittlement was the dynamic strain ageing effect.

3. The high-temperature deformation and fracture mechanism of ferritic spheroidal graphite cast irons showed the same tendency under the different stress conditions used in these tests. Nevertheless, it was always under the influence of strain rate.

References

1. K. CHICHIWA and M. HAYASHI, *IMONO* **51** (7) (1979) 395.
2. E. NECHTELBERGER, "Fachverlag Schiele und Schon Gmbh, Berlin, (1977) p. 442.
3. T. S. LUI and O. YANAGISAWA, *J. Foundry Ind. Taiwan* **36** (9) (1985) 1.
4. O. YANAGISAWA and T. S. LUI, *Metall. Trans. A* **16A** (1985) 667.
5. S. RIGGER, O. VOHRINGER and E. MACHERAUCH, *Gieserei Forsch.* **23** (1971) 35.
6. J. S. BLACKWORE and E. O. HALL: *Iron Steel Inst.* **8** (1966) 817.
7. T. S. LUI, Proceedings of the 2nd ROC-ROK Joint Workshop on Fracture of Metals (Tsing Hua University, Hsinchu, Taiwan, 1986) p. 297.
8. T. TAKEYAMA and H. TAKAHASHI, *Tetsu to Hagane* **58** (1972) 1054.
9. T. SAKII, M. OHASHI, M. KOZAI and S. SAKUI, *ibid.* **63** (1977) 124.
10. O. YANAGISAWA and T. S. LUI, *Trans. Jpn Inst. Metals* **12** (1983) 858.
11. C. E. JASKE, *Trans. ASME* (1977) 432.
12. M. OMORI, Y. YOSHINAGA and T. KAWAHATA, *Jpn Inst. Metals* **33** (1969) 730.
13. A. K. SACHDEV, *Met. Trans.* **13A** (1982) 1793.
14. M. ABE, *Jpn Inst. Metals* **45** (1981) 942.

Received 7 April
and accepted 5 September 1988